IEEE Access
Multidisciplinary | Rapid Review | Open Access Journal

Received 26 May 2023, accepted 27 June 2023, date of publication 5 July 2023, date of current version 21 July 2023.

Digital Object Identifier 10.1109/ACCESS.2023.3292791

RESEARCH ARTICLE

Collaborative Energy Management for Intelligent Connected Plug-In Hybrid Electric Vehicles Based on Autonomous Speed Planning

ZHENZHEN LEI[1], (Member, IEEE), YAFANG HUANG[1], SHUAI ZHANG[1], WENJUN WAN[1], YI SUI[1], AND YONGGANG LIU[2,3], (Senior Member, IEEE)

[1]School of Mechanical and Power Engineering, Chongqing University of Science and Technology, Chongqing 401331, China
[2]State Key Laboratory of Mechanical Transmissions, Chongqing University, Chongqing 400044, China
[3]College of Mechanical and Vehicle Engineering, Chongqing University, Chongqing 400044, China

Corresponding authors: Zhenzhen Lei (2010048@cqust.edu.cn) and Yonggang Liu (andyliuyg@cqu.edu.cn)

This work was supported in part by the National Natural Science Foundation of China under Grant 52002046, in part by the Chongqing Fundamental Research and Frontier Exploration Project under Grant CSTC2019JCYJ-MSXMX0076, and in part by the Chongqing University of Science and Technology Graduate Innovation Project under Grant YKJCX2220334.

ABSTRACT This paper proposes a collaborative optimization strategy for speed planning and energy management of intelligent plug-in hybrid electric vehicles (PHEVs). In this study, a single-axis parallel PHEV with the powertrain of P2 configuration is employed as the research object. Then, dynamic programming (DP) is leveraged to ensure optimal fuel economy with the consideration of the simultaneous optimal demand torque distribution and autonomous speed selection. An adjustment coefficient that reasonably constrains the feasible domain of vehicle speed is designed to limit the range of autonomous speed selection according to driving conditions. The reasonableness of speed selection is enhanced by adding penalty functions to inhibit gear shifting and speed fluctuations. To consider the variability of the control strategies based on the constraints of travel time and distance, a time-domain and a space-domain collaborative optimization model are established respectively, and a simulation analysis of the collaborative optimization energy management strategy is conducted. The simulation result shows that the strategy achieves the collaborative optimization of speed autonomous planning and reasonable allocation for demand torque. In addition, the proposed strategy demonstrates preferable energy economy under different constraints based on time and space domains.

INDEX TERMS Plug-in hybrid electric vehicles, collaborative optimization, energy management strategy, hierarchical optimization.

I. INTRODUCTION

With the increasing attention to environmental protection and energy conservation, clean energy vehicles with lower energy consumption and lighter emission pollution have become a research hotspot. Classical clean energy vehicles include electric vehicles (EVs), hybrid electric vehicles (HEVs) and fuel cell vehicles. EVs are regarded as an ideal solution to clean energy vehicles, due to the non-fuel consumption and pollutants, while the charging takes a relatively long time, and EV charging is not easy to be achieved due to the incomplete charging facilities [1]. HEVs are deployed with electric system and fuel system that can form different operation modes according to the power demand and vehicle dynamic state. Furthermore, PHEVs combine the merits of EVs and traditional HEVs to bring an all-electric range (AER) and featuring the characteristics of long driving range and high efficiency. Currently, PHEVs are one of the most promising solutions among clean energy vehicles [2]. With the wide development of perception, communication and automation technologies, PHEVs are gradually deployed with autonomous driving and connected capabilities that is referred to as intelligent connected PHEVs [3].

The associate editor coordinating the review of this manuscript and approving it for publication was Ricardo De Castro.

For PHEVs, an effective energy management strategy (EMS) is imperative to distribute the power between different energy sources, usually with the target of minimizing energy consumption under the premise of meeting the driving demand. EMSs are mainly divided into two categories which are rule-based and optimization-based strategies. Rule-based energy management strategies [4], [5] are both: 1) Deterministic rules identify heuristic functions based on human empirical values and form a control table to determine the energy allocation. A typical strategy is the charge-depletion and charge-sustaining (CD-CS) [6]. Fuzzy rules establish the affiliation function through expert experience and do not enable optimal control [7]. Reference [8] combines state of battery charge (SOC) and power limit to formulate an eco-discharge strategy that offers better fuel economy than the CD-CS strategy. Although rule-based strategy features strong practicality, it heavily relies on empirical engineering practice and is difficult to attain the optimal solution, especially when encountering time-varying driving conditions.

Optimization-based strategies are mainly divided into global optimization methods and instantaneous optimization solutions [9]. Dynamic programming (DP) has been widely adopted so far as a typical global optimization strategy [10]. However, DP requires detailed power demand in the whole optimization range which is more preferred to offline application because of time and space consuming when applying for energy management of PHEVs. Therefore, the solution of DP is generally considered as an ideal benchmark to evaluate the performance of other algorithms of energy management [11]. Reference [12] adopts the DP algorithm for global optimization to obtain the optimal torque distribution under historical operating conditions provides the application guideline for online implementation. On the other hand, the representative strategies for instantaneous optimization are model predictive control (MPC) and equivalent consumption minimization strategy (ECMS) [13], [14]. Reference [15] formulates an MPC strategy based on an evolved EMS to rationally distribute the demand power of the PHEV among multiple power sources. In [16], an EMS incorporates real-time traffic information is proposed with an equivalence factor (EF) that can be dynamically adjusted according to operation conditions. In [17], [18], [19], [20], and [21], adaptive ECMS (A-ECMS) is designed according to different driving conditions to achieve energy savings of PHEVs.

With the development of intelligent connected techniques [22], the vehicle speed is planned after absorbing the surrounding road and neighbor vehicle information. In a hierarchical control strategy the upper layer plans the speed based on the driving conditions and intelligent traffic data and the lower layer allocates the demand power based on the predicted speed information derived in the upper layer [23]. Reference [24] describes the upper layer solves the optimal driving speed with a fuzzy adaptive algorithm, and the lower layer using an A-ECMS combined with a genetic algorithm (GA) to optimize power allocation to increase fuel economy. Reference [25] proposes an A-ECMS combining Markov chains and back propagation (BP) neutral networks to predict vehicle speed, reasonably select driving modes and accomplish power allocation. Reference [26] leverages the radial basis function neural network algorithm to predict SOC to obtain predictive EMS (PEMS).

The conventional PHEV EMS is based on the hierarchical control of driving factors which does not sufficiently consider the influence of vehicle speed on energy management and is unable to achieve the optimal control of the integrated vehicle energy. In this paper, a collaborative optimization study is conducted on the autonomous selection of vehicle speed and real-time torque distribution of power source for intelligent networked PHEVs to effectively reduce the cost of integrated energy consumption. The contributions of this paper are mainly embodied in the following two perspectives: 1) An adjustment factor that properly constrains the feasible domain of vehicle speed is designed to study the collaborative optimization of vehicle speed autonomous selection and power source demand torque distribution in real time according to the driving condition limitation range. 2) The DP optimization method is used to solve the proposed collaborative control strategy in this paper. The remainder of this paper is organized as follows: In Section II, the vehicle model is established and addressed. In Section III, the speed feasible region design rule is illustrated, and the design of an optimal energy management strategy based on DP is completed. In Section IV, the feasibility of the collaborative optimization strategy is verified, and the simulation results are compared. In Section V, the conclusions of this paper are presented.

II. POWERTRAIN CONFIGURATION AND SYSTEM MODELING

In this paper, a PHEV equipped with single-axis parallel P2 configuration is selected as the research object, and the design of the vehicle drive scheme is shown in Fig. 1. As can be found, the powertrain is mainly composed of five key components, i.e., engine, motor, dual clutch transmission (DCT) gearbox, main reducer, main clutch and battery pack. The motor can be a generator to store energy for the battery or an electric motor to propel the wheels. The DCT clutch is a double clutch without internal torque converter and planetary

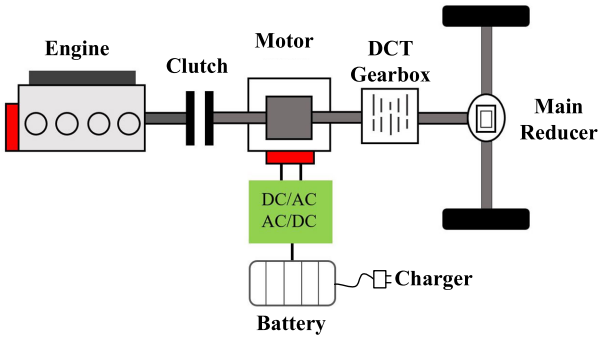

FIGURE 1. PHEV powertrain.

gear set. The DCT transmission is comprised of two clutches, one handling even gears and the other handling odd gears.

A. ENGINE MODEL

The main input to the model of the engine mainly includes output torque, speed, throttle opening, etc. [27]. According to the bench test data, the engine fuel consumption model can be established, as:

$$T_e = f(n_e, \alpha) \tag{1}$$
$$b_f = f(T_e, n_e) \tag{2}$$

where T_e is the output torque of the engine, b_f denotes the fuel consumption, n_e means the engine speed, and α represents the throttle opening. The operational performance of the components was obtained using bench experimental data and modeled in MATLAB simulation as shown in Fig. 2 (a) and Fig. 2 (b). The maximum torque of the engine is 300Nm and the maximum power is 150kW. The image data matched the above requirements which will allow the engine to work more efficiently and the parameters set to meet the requirements.

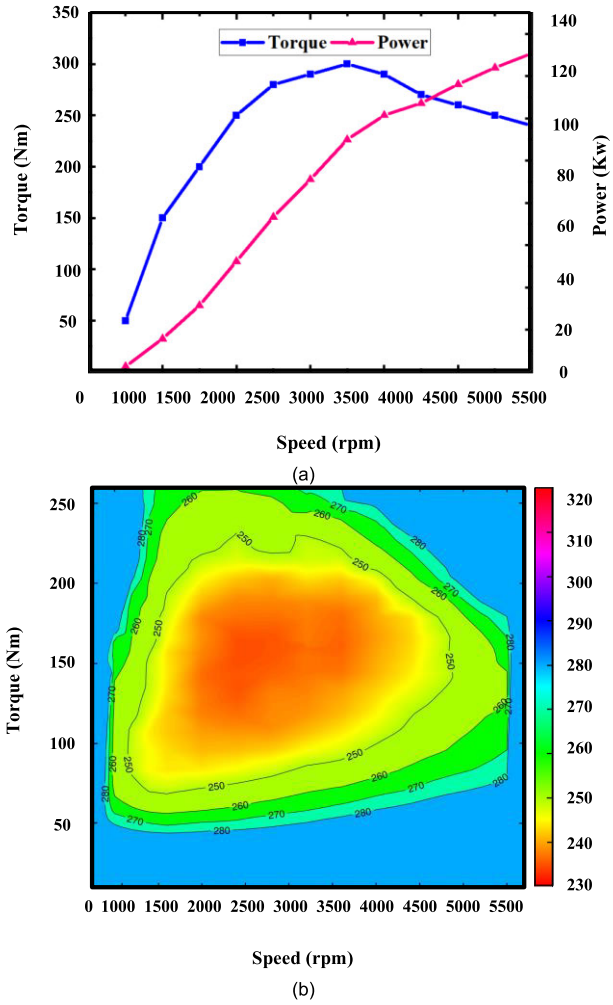

FIGURE 2. Engine model. (a) External characteristic curves of the engine. (b) Fuel consumption of the engine.

B. MOTOR MODEL

The main input parameters of the deployed ISG model mainly include motor torque, motor speed and motor efficiency. The efficiency and power of the motor are calculated, as:

$$\eta_m = f(n_m, T_m) \tag{3}$$
$$p_m = \eta_m T_m n_m \tag{4}$$

where η_m indicates motor efficiency, n_m denotes motor speed, T_m represents motor torque, P_m indicates motor power, and n_m means motor speed. The maximum torque of the motor is 140Nm and the maximum power is 50kW. The external characteristic curves in Fig. 3 (a) and efficiency diagram of motor is demonstrated in Fig. 3 (b) which is in a range of torque limitation and the motor efficiency is good.

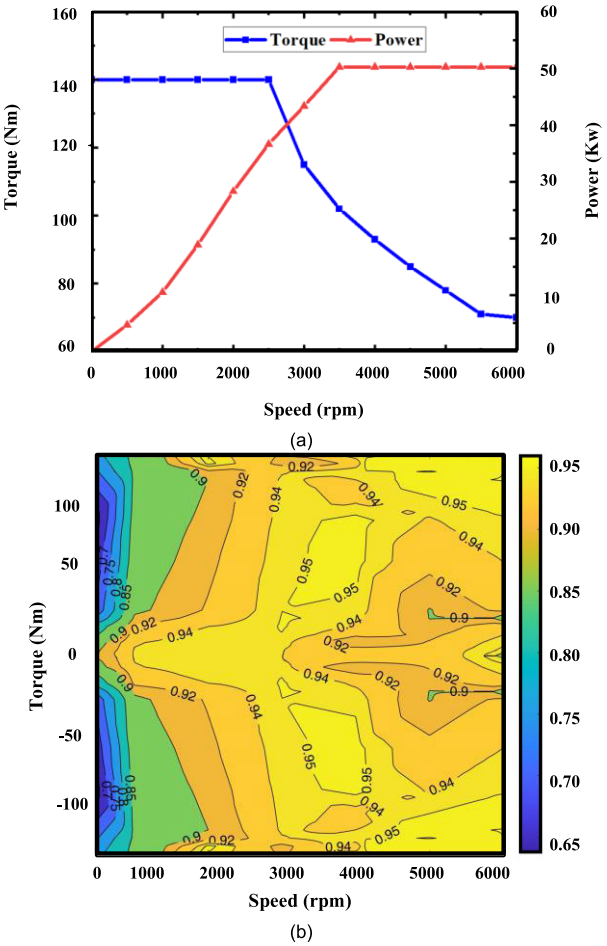

FIGURE 3. ISG model. (a) External characteristic curves of motor. (b) efficiency diagram of motor.

C. BATTERY MODEL

In this paper, a simplified battery model is established which consists of a resistor and an open voltage source [28]. The effects of temperature and aging on internal resistance are ignored. The relationship between battery resistance, electric potential and SOC can be obtained by interpolation

fitting, and the theoretical representation can be determined as follows:

$$P_b = I \cdot U \tag{5}$$

$$U = E - IR \tag{6}$$

$$I = \frac{E - \sqrt{E^2 - 4RP_b}}{2R} \tag{7}$$

where P_b is the battery power, I means battery current, E stands for electromotive force, U is the termination voltage, and R representatives equivalent resistance.

The SOC estimation method of the battery is calculated by the current integration method with the initial value of SOC and the battery current for the battery charge state shown as follow:

$$SOC(t) = SOC(t_0) - \frac{\int_{t_0}^{t} i(t)dt}{C} \tag{8}$$

where t stands for the t^{th} moment, t_0 represents the initial moment, $SOC(t)$ means the state of charge of the battery at the t^{th} moment, $SOC(t_0)$ denotes the value of SOC at the initial moment, $i(t)$ indicates the current at t^{th} time,and C is the battery capacity. As shown in Fig.4 (a) and Fig.4 (b), the internal resistance and voltage of the battery vary with the direction of current, and the specific data are obtained from the bench test.

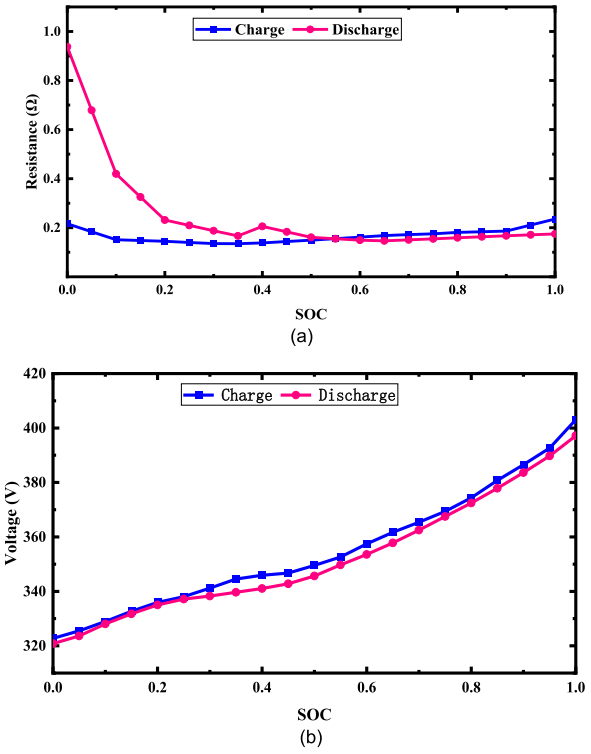

FIGURE 4. Battery model. (a) Curves of battery charging and discharging resistance and SOC. (b) Battery charge and discharge electromotive force and SOC change curves.

III. COLLABRATED OPTIMIZATION ENERGY MANAGEMENT STRATEGY

In this article, a collaborative optimization based on autonomous speed planning is proposed, and the design flow is shown in Fig.5. As can be seen, collaborative optimization is based on from the following three points. Firstly, the boundary factor is added to set the rule feasible domain to determine the working conditions which is closer to actual road requirement criteria. Secondly, the DP method stores the optimal paths of each stage and reduces the repeated calculations compared with the conventional algorithm. Thirdly, the coupling relationship between autonomous speed planning and torque distribution is considered to design a collaborative optimization strategy.

A. COLLABORATIVE OPTIMIZATION MODEL IN TIME DOMAIN

The collaborative optimization model is solved based on the dynamic programming algorithm, and the process of structural design and parameter setting is basically the same as the way of solving the dynamic programming problem. When discussed from the time domain, the driving task is measured in terms of time duration which is determined but the driving distance is not constrained. The opposite is true when discussing from the space domain, where driving under the distance constraint does not ensure the duration of time. Discussing from different constraints, firstly, it can be determined that the synergistic strategy can complete the driving task with generality in different angles of limitation states. Then, the loss of driving distance and time can be derived from the comparison between the results of synergistic optimization in time and space domain and the results of hierarchical optimization. The foundation is laid for the subsequent addition of the boundary adjustment factor of the feasible domain to limit the driving range of the vehicle speed autonomy selection. In this paper, we will conduct a comparative analysis and research on collaborative optimization from the above two aspects.

1) CONSTRUCTION MODEL

The time step is set as a stage variable with 1 s as an incremental step. The engine torque, gear shift speed ratio and acceleration are selected as decision variables, as:

$$u(k) = f(T_e, i_{DCT}, a) \tag{9}$$

where $u(k)$ stands for the decision variable, k means the k stage, a represents the acceleration of the k stage, v_f represents the discrete speed in the finale place after the k stage of dispersion, and v_a represents the discrete speed in the first place after the k stage of dispersion.

$$\begin{cases} x(k+1) = f(x(k), u(k), k) \\ x(0) = x_0 \end{cases} \tag{10}$$

The state variables are time, vehicle speed and SOC. Where, $x(k+1)$ means the $k+1$ state of the power battery

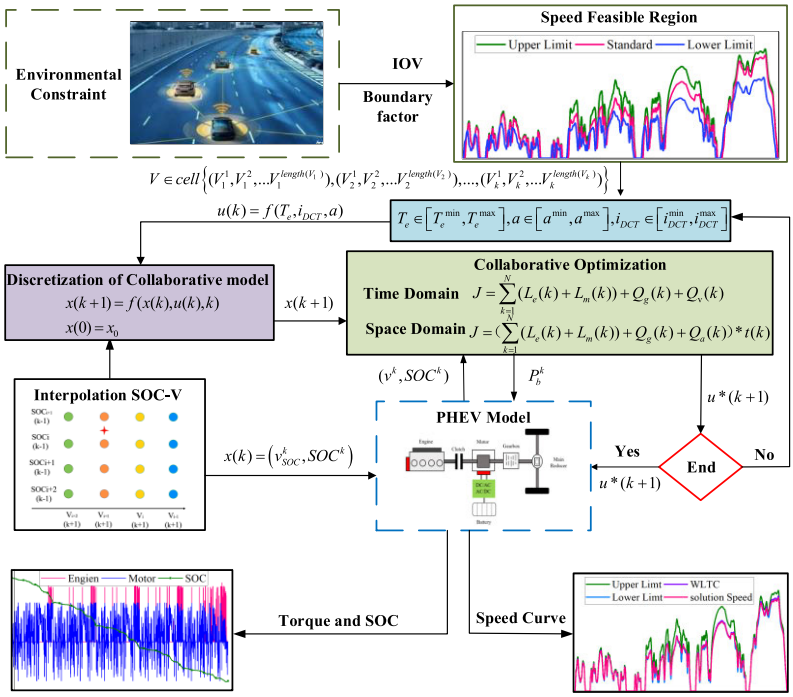

FIGURE 5. Collaborative optimization design process.

SOC and vehicle speed, $x(k)$ represents the k state of the power battery SOC and vehicle speed, $u(k)$ stands for the decision variable in the kth phase, $x(0)$ indicates the initial value of SOC and vehicle speed and is assigned to x_0.

The constraints are shown in (11). The DCT transmission follows the rules of sequential upshift and interval downshift when shifting. Secondly, in order to ensure that the vehicle autonomous speed planning results satisfy the actual driving, the acceleration, speed and speed transfer vectors are restricted as shown in (12). Finally, two penalty functions are added to the collaborative optimization. The same vehicle speed could correspond to different gears, and the frequent shifting due to speed changes can lead to loss of energy consumption and wear of operating components. To enhance economy and ensure smoothness of the shift penalty function is considered, as formulated in (13). Penalty values are obtained using the enumeration method. A penalty function is taken into consideration to suppress the invalid speed change and obtain smooth speed curves when vehicle speed is autonomously planned, as shown in (14).

$$\begin{cases} T_{e\,\min} \le T_e \le T_{e\,\max} \\ T_{m\,\min} \le T_m \le T_{m\,\max} \\ 0 \le n_e \le n_{e\,\max} \\ n_{m\,\min} \le n_m \le n_{m\,\max} \\ SOC_{\min} \le SOC(k) \le SOC_{\max} \\ i_{DCT\min} \le i_{DCT}(k) \le i_{DCT\max} \end{cases} \tag{11}$$

where $T_{e\max}$ and $T_{e\min}$ mean the maximum and minimum engine torque respectively, $n_{e\max}$ and $n_{m\min}$ indicate the maximum and minimum engine speed, $T_{m\max}$ and $T_{m\min}$ denote the maximum and minimum torque of the motor, $n_{m\max}$ and $n_{m\min}$ stand for the maximum and minimum speed of the motor, $SOC_{\max}$ and $SOC_{\min}$ represent the maximum and minimum of SOC, respectively, $i_{DCT\max}$ and $i_{DCT\min}$ respectively represent the highest, lowest gear, $i_{DCT}(k)$ and $i_{DCT}(k+1)$ represent the $k, k+1$ time gear value.

$$\begin{cases} vm(k) \le v(k) \le vM(k) \\ vm(k+1) \le vo(k) \le vM(k+1) \\ am \le a(k) \le aM \end{cases} \tag{12}$$

where $v(k)$ signifies the state variable of the kth stage speed, $vM(k)$ and $vm(k)$ represent the maximum speed and minimum speed in the k^{th} stage, $vo(k)$ denotes the selectable range of speed for k^{th} stage, $a(k)$ shows the state variable of the k^{th} stage acceleration, am, and aM indicates the maximum and minimum acceleration at the k^{th} moment.

$$Q_g(k) = \begin{cases} 0 \\ 0.0008 \\ NAN \end{cases} \tag{13}$$

$$Q_{\text{v}}(k) = \begin{cases} (abs(V_c - V_o))V_p \\ 0 \end{cases} \tag{14}$$

where $Q_g(k)$ shows the gear penalty function at time k, $Q_{\text{v}}(k)$ denotes the penalty function for speed fluctuations at time k, V_O indicates the speed selectable value at time k, V_C represents the initial speed matrix at the next time, and V_P means the penalty value. After satisfying the above constraints, the

time domain objective function can be expressed as:

$$\begin{aligned} J &= \sum_{k=1}^{N} L(x(k), u(k)) \\ &= \sum_{k=1}^{N} (p_f Q_e(k) + p_m Q_m(k)) + Q_g(k) + Q_{\mathrm{v}}(k) \end{aligned} \tag{15}$$

where J means the comprehensive cost, p_f represents the unit price of fuel, $Q_e(k)$ is the fuel consumption at time k, p_m represents the unit price of electric energy, and $Q_m(k)$ represents the electricity consumption at time k.

2) SOLVING MODEL

The PHEV is solved in the time domain by the DP, but its state variable vehicle speed becomes an indefinite variable. The ordinary two-dimensional matrix can no longer meet the system design requirements, the state variable needs to be stored using a three-dimensional matrix. It makes the computation highly inefficient, and the storage capacity is so large that the computer does not work efficiently. The cell array technique can effectively raise the storage space, increase the computation speed, and reduce the computer performance requirements [29]. The variable matrix storage size and representation can be calculated as:

$$\begin{cases} cell(1, Lt) \\ size(Ls, La(k)) \end{cases} \tag{16}$$

The initial and final velocity matrix magnitudes are expressed, as:

$$\begin{cases} vf = size(1, Lf(k)) \\ va = size(1, La(k)) \end{cases} \tag{17}$$

The cost is expressed as:

$$\begin{cases} J = cell(1, Lt) \\ J\{k\} = size(Ls, La(k)) \end{cases} \tag{18}$$

The size of the matrix of decision variables is expressed, as:

$$\begin{cases} size[La(k), Lf(k)] \\ size[La(k), Lf(k), Lg, Lu] \end{cases} \tag{19}$$

where V is the velocity state variable, A indicates the acceleration decision variable, G denotes the state variable of the gear decision, U stands for the torque decision state variable, J is the total cost, Lt indicates the length of the stage, $La(k)$ means the length of the initial velocity at the k stage; Ls is used as the discrete length of the SOC, vf shows the end dispersion matrix of the velocity at a certain stage, $Lf(k)$ denotes the size of the end dispersion matrix of the velocity at a certain stage, va indicates the velocity at a certain stage denotes the initial dispersion matrix, $La(k)$ represents the size of the initial dispersion matrix and the size of the matrix at the k^{th} moment is $size(Ls, La(k))$.

Not all values within the velocity and acceleration domain are adequate to full satisfy the collaborative optimization requirements. The process of selecting data is as follow:

$$\begin{cases} pt = find(\tilde{}isnan(v)) \\ [c1, c2] = ind2sub\{(La, Lf), pt\} \\ c1 = unique(c1) \\ c2 = unique(c2) \\ V\{i\} = va(c1) \\ vs(c2) = c2 \\ vi = repmat(vs, La, 1, Lg, Lu) \end{cases} \tag{20}$$

where vs indicates the speed matrix corresponding to the SOC state; vi denotes the speed matrix of the interpolation. If the value of the current speed is not found within the acceleration threshold to reach the next stage properly, the data will be removed as invalid points. Then the valid data will be stored to obtain the decision variables and interpolated values.

The solution process still follows the principle of sub-problem optimality, and the expression is shown in (21). The state variables in the next stage of the forward optimization search process are represented, as shown in (22).

$$\begin{cases} J^*(x(k)) = \min\limits_{u(k)}[L(x(k), u(k))] + J^*(x(k+1)) \\ x(k+1) = f(x_k, u(x_k)) \end{cases} \tag{21}$$

$$\begin{cases} vn(k+1) = vn(k) + an(k) \\ SOC(k+1) = SOC(k) \\ \quad - \dfrac{U(SOC) - \sqrt{U(SOC)^2 - 4R(SOC)P_{\mathrm{m}}(k)}}{2R(SOC)C} \end{cases} \tag{22}$$

where J^* denotes instantaneous cost, $vn(k+1)$ means the speed of the $k+1^{\mathrm{th}}$, $vn(k)$, $an(k)$ and $P_{\mathrm{m}}(k)$ is the velocity, acceleration and motor power of k. During the solution of the system, the solution of the previous stage possibly cannot fall exactly on the grid points of the state variables for which the discretization is complete. As the speed becomes variable, the interpolation point changes from single data to coupled data SOC-V. The interpolation solution procedure is shown in in Fig. 6 (a) and Fig. 6 (b).

B. COLLABORATIVE OPTIMIZATION MODEL IN SPACE DOMAIN

1) CONSTRUCTION MODEL

In using distance as a uniform discretization of the phase, the integrity of the mileage is broken, and the speed appears to be stepwise. In this paper, the space domain collaborative optimization model uses with non-uniform discrete distances as stages while planning the vehicle speed in a range of given speeds. The decision functions remain the same as before including vehicle acceleration, engine torque and gear position. The state transfer function and state variables are driving range, vehicle speed and battery SOC. The constraints, shift penalty, and velocity fluctuation penalty are consistent with

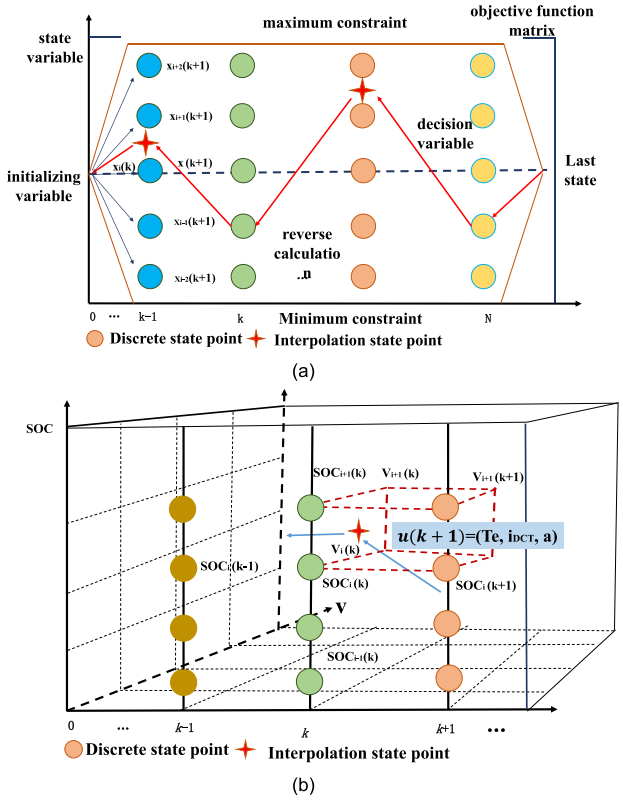

FIGURE 6. The procedure of interpolation solution.

those of the time-domain rules. The time factor is added in the design of the objective function as follows:

$$J = \sum_{k=1}^{N} L(x(k), u(k)) = (\sum_{k=1}^{N} (p_f Q_e(k) + p_m Q_m(k)) + Q_g(k) + Q_v(k))^* t(k) \tag{23}$$

where t denotes the time passed in the k^{th} period.

2) SOLVING MODEL

The solution steps in the space domain are similar to the time domain, and the data with space domain characteristics are stored. The variable matrix is stored, as:

$$\begin{cases} cell(1, Ld) \\ size(Ls, La(k)) \end{cases} \tag{24}$$

The initial and final velocity matrices are expressed as:

$$\begin{cases} vf = size(1, Lf(k)) \\ va = size(1, La(k)) \end{cases} \tag{25}$$

The costs are transformed into:

$$\begin{cases} J = cell(1, Ld) \\ J\{k\} = size(Ls, La(k)) \end{cases} \tag{26}$$

The matrix of decision variables is expressed as:

$$\begin{cases} size[La(k), Lf(k)] \\ size[La(k), Lf(k), Lg, Lu] \end{cases} \tag{27}$$

The non-uniformly discrete spatial domain phases are constrained in their selection using the travel distance of each phase in the time domain. Therefore, the non-uniformly discrete distance space domain model has the same driving distance with the uniformly discrete time model at the same horizontal coordinate. The relationship between driving time, distance, and speed is as follow.

$$\begin{cases} d\_d(k+1) = d\_d(k) + v(k) + \dfrac{v(k+1) - v(k)}{2} \\ a = ((vf)^2 - (va)^2)/(2 * d\_d(k)) \\ t = (2 * d\_d(k))/(vf + va) \end{cases} \tag{28}$$

where Ld refers to the discrete distance length, $v(k)$, $v(k+1)$ stands for the average velocity of stage k^{th}, $k{+}1^{\text{th}}$, and $d\_d(k+1)$ indicates the mileage of stage $k+1^{\text{th}}$.

C. SPEED LIMITED DRIVING CYCLES

During the simulation, it is found that the smaller the value of the adjustment factor of the lower limit for feasible domain is taken, the better the economy. In contrast to standard working condition data, vehicles in the time domain fail to reach their destination within the specified time and take more time in the space domain resulting in non-corresponding demand. To combine the economy, driving time and distance constraints, an adjustment factor α is added to constrain the feasible domain of the speed, as:

$$\begin{cases} V_u = \alpha_u V \\ V_l = \alpha_l V \\ \alpha_u > 0 \\ 0 < \alpha_l < 1 \end{cases} \tag{29}$$

where V represents the original speed data value, V_u stands for the upper speed limit after constraint, V_l means the lower speed limit after constraint, the value of the upper bound constraint is represented by α_u, and the lower bound constraint factor takes the value α_l.

The world light vehicle test cycle (WLTC) as an example of collaborative optimization simulation analysis. The feasible range of autonomous speed planning is important for the speed pick-up, energy economy, driving time and distance of intelligent connected plug-in hybrid vehicles. The higher the adjustment factor of the upper limit of the feasible domain, the better the economy. Therefore, the upper limit of the feasible domain is adjusted by an upper limit factor based on the maximum speed set for each country for different road sections. Therefore, this paper constrains the four working conditions stages of WLTC: low speed, medium speed, high speed and ultra-high speed according to the road driving speed limit conditions respectively takes the highest speed of each stage as the standard to ensure the speed feasible domain meets the actual requirements. The maximum speed limits of the above four stages are 140km/h, 100km/h, 90km/h and

60km/h. The constraint functions for the velocity domain of each interval are expressed as follows:

$$\begin{cases} V_u^1 = \alpha_u^1 V_l \\ V_u^2 = \alpha_u^2 V_m \\ V_u^3 = \alpha_u^3 V_h \\ V_u^4 = \alpha_u^4 V_u \\ V_1 = \alpha_l V \end{cases} \tag{30}$$

The simulation results are more in line with the combined travel time and distance requirements of the exhaustive approach in the lower bound constraint factor is 0.98 or above. Therefore, in this paper, α_l is 0.98 as an example for analysis and illustration. To achieve a comparison effect, the plots of the space data for the selected 0.9 are presented in section IV for comparison and illustration. The final choice of speed equation is shown below: V_l, V_{m}, V_{h} and V_{u} represent the raw data in the low speed, medium speed, high speed and ultra-high speed of stage speed data of WLTC. Where V_u^1, V_u^2, V_u^3, and V_u^4 represent the maximum speed that can be reached after setting the rule limit, respectively, the specific parameters are shown in TABLE 1.

TABLE 1. Speed feasible domain rule table.

Driving cycle	Max-V (km/h)	Upper limits (km/h)	Constraint factor
City (Low speed)	57.0	60.0	1.06
Suburban (Medium speed)	75.0	90.0	1.30
Rural (High speed)	83.0	100.0	1.20
Highways (Ultra-high speed)	131.1	140.0	1.06

The corresponding speed data in the time domain and space domain are shown in Fig. 7 (a) and Fig. 7 (b).

EMSs for vehicles have been studied in a much more uniform way with respect to time domain based on international open-source information given with standard working condition data in the speed-time data for simulation calculations. Artificially setting the standard design space domain is simpler when dealing with driving conditions, but can result in incomplete driving conditions. It is difficult to judge the correctness due to different standards, and there is a travel loss error. The time domain working condition is directly transformed into the space domain which has stronger mathematical logic, more rational, rigorous and convenient characteristics. Therefore, this paper conducts a simulation analysis study based on the latter. In this paper, the collaborative optimization is designed in an inhomogeneous and discrete way to avoid speed steps and driving conditions irregularities. The point with zero-speed in the time domain is zero-distance in the space domain which cannot be displayed on the speed-distance data plot. The data points generated in this case are called invalid points which have been removed for graphical simplicity purposes.

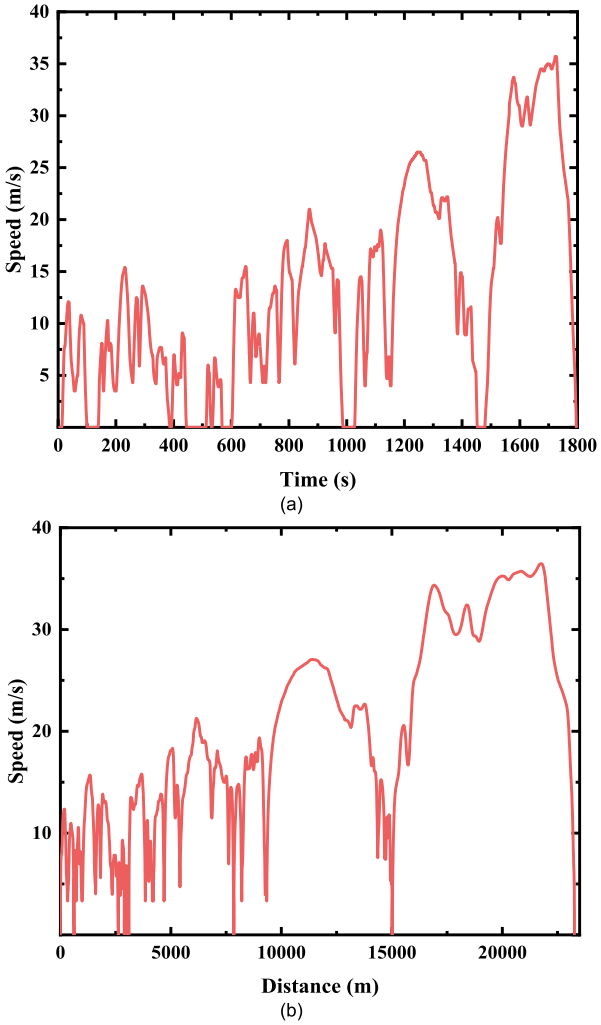

FIGURE 7. WLTC cycle. (a) Time. (b) Space.

IV. RESULTS AND ANALYSIS

To validate the rationality of the collaborative optimization, a simulation study of a parallel hybrid vehicle is conducted with the specific parameters of the vehicle as shown in TABLE 2. In this paper, simulation is verified in both time and space domains, and the SOC threshold of this strategy is chosen to be 0.8 to 0.2 to give full play to the economic advantages of the electrical system.

A. TIME DOMAIN

The test range is 5 WLTC driving cycles. Since the mileage is long enough, the autonomous vehicle will go into mixed mode and the results are shown in Fig. 8 to Fig. 10. The time domain autonomous speed planning curve is close to the lower limit. Acceleration and deceleration are performed in advance at the acceleration mutation point which makes the absolute value of acceleration smaller. As a result, speed changes are more rational, and the reduced frequency of gear changes allows for increased energy economy.

The distributions of torque and SOC are shown in Fig. 11. The battery releases energy uniformly throughout the

TABLE 2. Vehicle parameters and vehicle objectives.

Item	Parameter	Value
Vehicle parameters	Readiness mass (Kg)	1885
	Windward area (A/m^2)	2.68
	wind resistance coefficient-Cd	0.34
	Wheel radius (r/m)	0.36
	Rolling resistance coefficient-f	0.0075
Engine	Maximum speed (km/h)	131.30
	Rated power (kW)	120
	Peak power (kW)	150
	Maximum speed (r·min^{-1})	5700
	Rated torsion (Nm)	286
	Peak torque (Nm)	300
Motor	Rated power (kW)	35
	Peak power (kW)	50
	Motor base speed (r·min^{-1})	3000
	Maximum speed (r·min^{-1})	6000
	Rated torque (Nm)	120
	Peak torque (Nm)	140
Battery	Standard voltage (V)	350
	Maximum battery capacity (kWh)	70
DCT	1-6 gear ratio i1/i2/i3/i4/i5/i6	3.917/2.429 /1.436/1.021 /0.848/0.667
	Main reducer speed ratio ia1/ia2	3.762/4.158

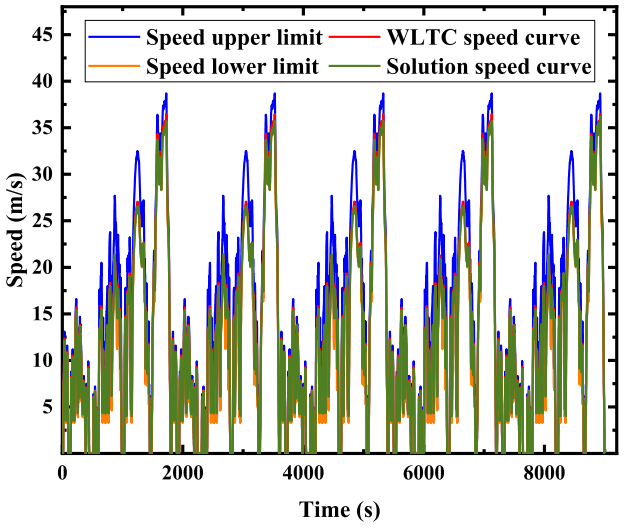

FIGURE 8. Speed comparison of 5 WLTC in Time.

process, with the SOC curve showing a uniform downward trend within the allowed range. The curve of SOC tends to a higher level. The reasonable distribution mode makes the engine work in a more moderate load state.

B. SPACE DOMAIN

The strategy is solved in space domain using in the same working conditions restrictions. The speed autonomous

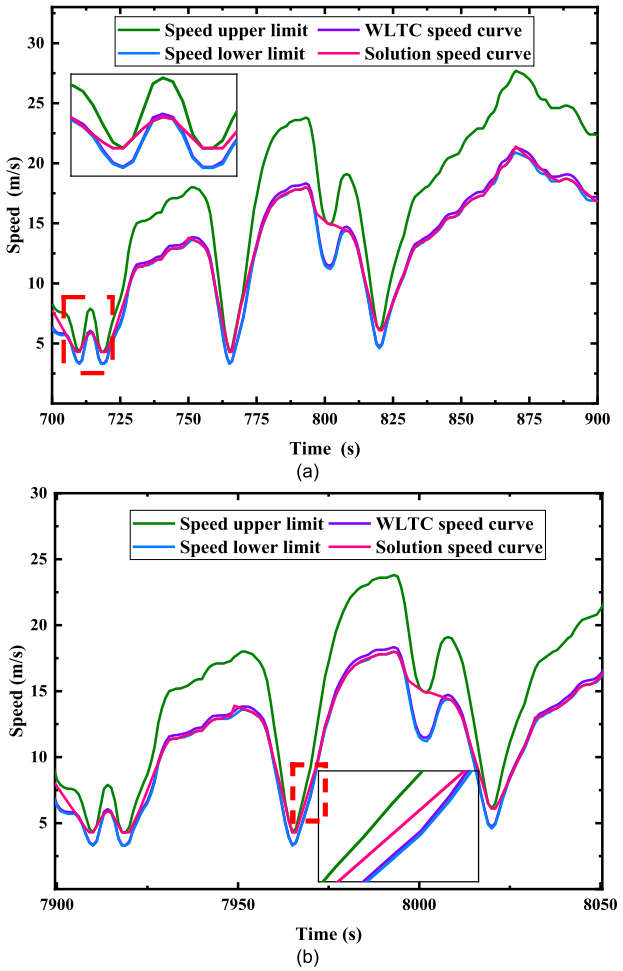

FIGURE 9. Partial magnification of speed of 5 WLTC in Time. (a) 700-900s. (b)7900-8050s.

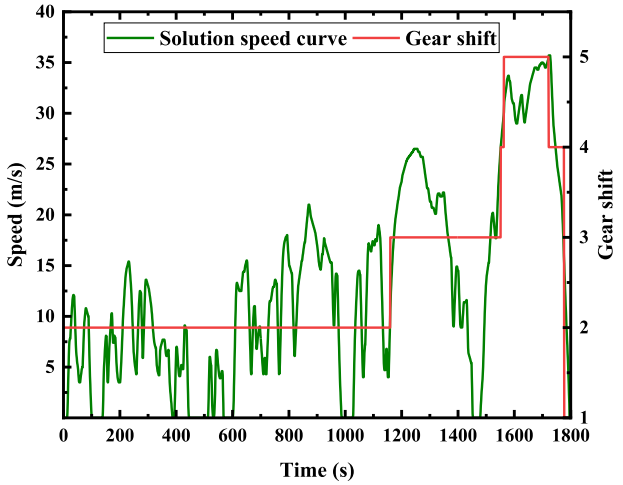

FIGURE 10. Comparison diagram of speed and gear of 1 WLTC cycle in Time.

planning curve shown in Fig.12 and is also close to the downlink driving limit. The underlying trends are similar in the time domain. The gear shifting in Fig.14 meets the reality

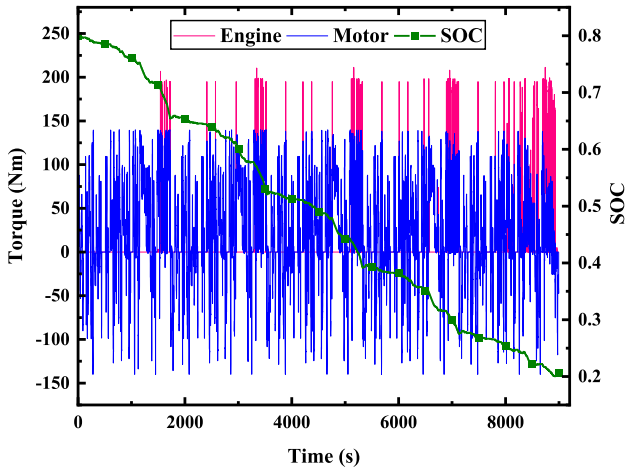

FIGURE 11. Engine, motor torque and SOC curves of 5 WLTC in Time.

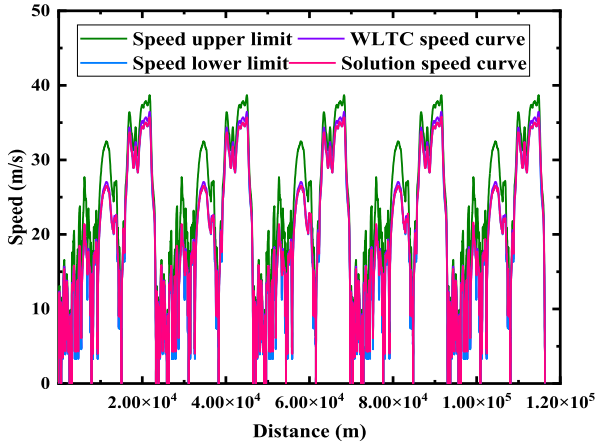

FIGURE 12. Speed comparison of 5 WLTC in Space.

of driving requirements. As shown in Fig. 13 (a), Fig. 13 (b) and Fig. 15, the high gear stage in the gear-speed comparison diagram is more than in the time domain. In the torque and SOC comparison plots, the energy is released uniformly by the battery. Motor is still involved for the entire driving range. The engine operates at a higher frequency than in the time domain.

From the simulation results of time domain and space domain, it can be seen that the focus of the two is different. The vehicle speed is planned autonomously in time domain, economy is preferred, the simulation is completed by stopping within the specified time. The driving process is not constrained by the mileage. The average speed is smaller, and the speed curve is smoother. The results of space domain are done with economy as a prerequisite for distance, the vehicle is not constrained by time. Average speed is relatively high, and the economy is slightly worse than in the space domain. Both simulation results are less economical than the original velocity curves.

In engineering practice, both distance and time are important for passengers. The co-optimization strategy is validated in both time and space domains. After adding the speed

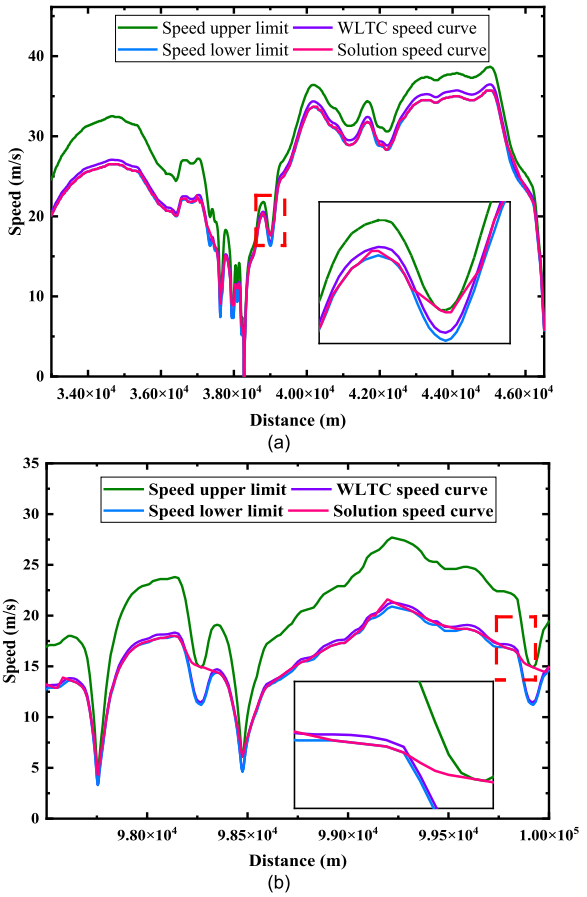

FIGURE 13. Partial magnification of speed of 5 WLTC in Distance. (a) 3.30 × 10^3-4.65 × 10^4m. (b) 9.75 × 10^3-1.00 × 10^5m.

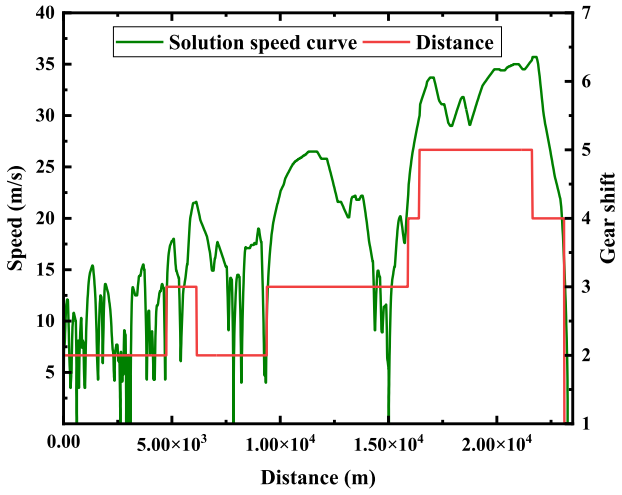

FIGURE 14. Comparison diagram of speed and gear of 1 WLTC cycle in Space.

domain adjustable factor, it can take into account both of them which proves its feasibility and practical application.

C. LOWER LIMIT VALUE COMPARISON SIMULATION

The option of speed feasible region in collaborative optimization management strategy is crucial. Since the maximum

TABLE 3. Time domain planning and hierarchical optimization cost analysis.

Control strategy	Fuel consumption	Electricity consumption	Costs	Distance	Time
	CNY	CNY	CNY	km	s
Cooperation optimization	5.50	8.00	13.50	107.10	9000
Hierarchical optimization	16.30	8.20	24.50	116.33	9000

TABLE 4. Space domain planning and hierarchical optimization cost analysis.

Control strategy	Fuel consumption	Electricity consumption	Costs	Distance	Time
	CNY	CNY	CNY	km	s
Cooperation optimization	9.00	8.00	17.00	116.33	9442
Hierarchical optimization	16.30	8.20	24.50	116.33	9000

TABLE 5. Time domain planning and hierarchical optimization cost analysis.

Control strategy	Fuel consumption	Electricity consumption	Costs	Distance	Time
	CNY	CNY	CNY	km	s
Cooperation optimization	13.80	8.00	21.8	115.86	9000
Hierarchical optimization	16.30	8.20	24.50	116.33	9000

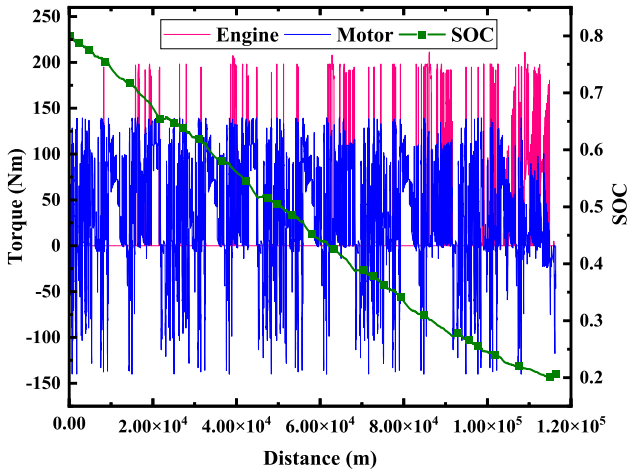

FIGURE 15. Engine, motor torque and SOC curves of 5 WLTC in Space.

velocity is used as the upper bound in the space domain to select the value of the adjustment factor with better economy, the choice of its value is not discussed in further detail. Unreasonably low speed limits are set to achieve energy savings, but they do not balance travel time and distance.

To verify the accuracy of the adjustment factor of the lower speed limit value adopted in this paper, simulated data with a lower limit constraint factor α_l of 0.9 is used as an example. The simulation results indicate that the operating, the working conditions of the time domain and the space domain are shown in Fig. 16 (a) to Fig. 16 (d). In Fig. 16 (a) and Fig. 16 (b), the PHEV is in pure electric operation mode at 1 WLTC, and the engine is not assigned torque at that stage. As shown in Fig. 16 (c) and Fig. 16 (d), the results at 5 WLTC demonstrate that the engine operating frequency decreases significantly. The slope of the battery SOC curve becomes smaller, and the energy of battery is released more slowly compared to the case where the adjustment factor α_l takes the value of 0.98.

D. COST AND EFFICIENCY

In this paper, a hierarchical EMS based on DP is designed to further investigate and analyze the accuracy of the collaborative optimal energy management strategy. For simulations of strategies based on the same constraints, at WLTC cyclic operating conditions the following results are obtained for the WLTC periodic operating conditions. For the economic analysis, the currency unit is chosen as China Yuan (CNY).

The results for the adjustable factor of 0.90 for the lower limit of the speed domain are shown in Tables TABLE 3 and TABLE 4. It shows a 44.9% increase in economy compared to the hierarchical optimized time domain, but with 9.3 km less driving distance. The economy in the space domain was improved by 30.7%, with an additional 442 seconds of time consumed. As shown in Tables TABLE 5 and TABLE 6, α_l is selected as 0.98. Compared to the hierarchical

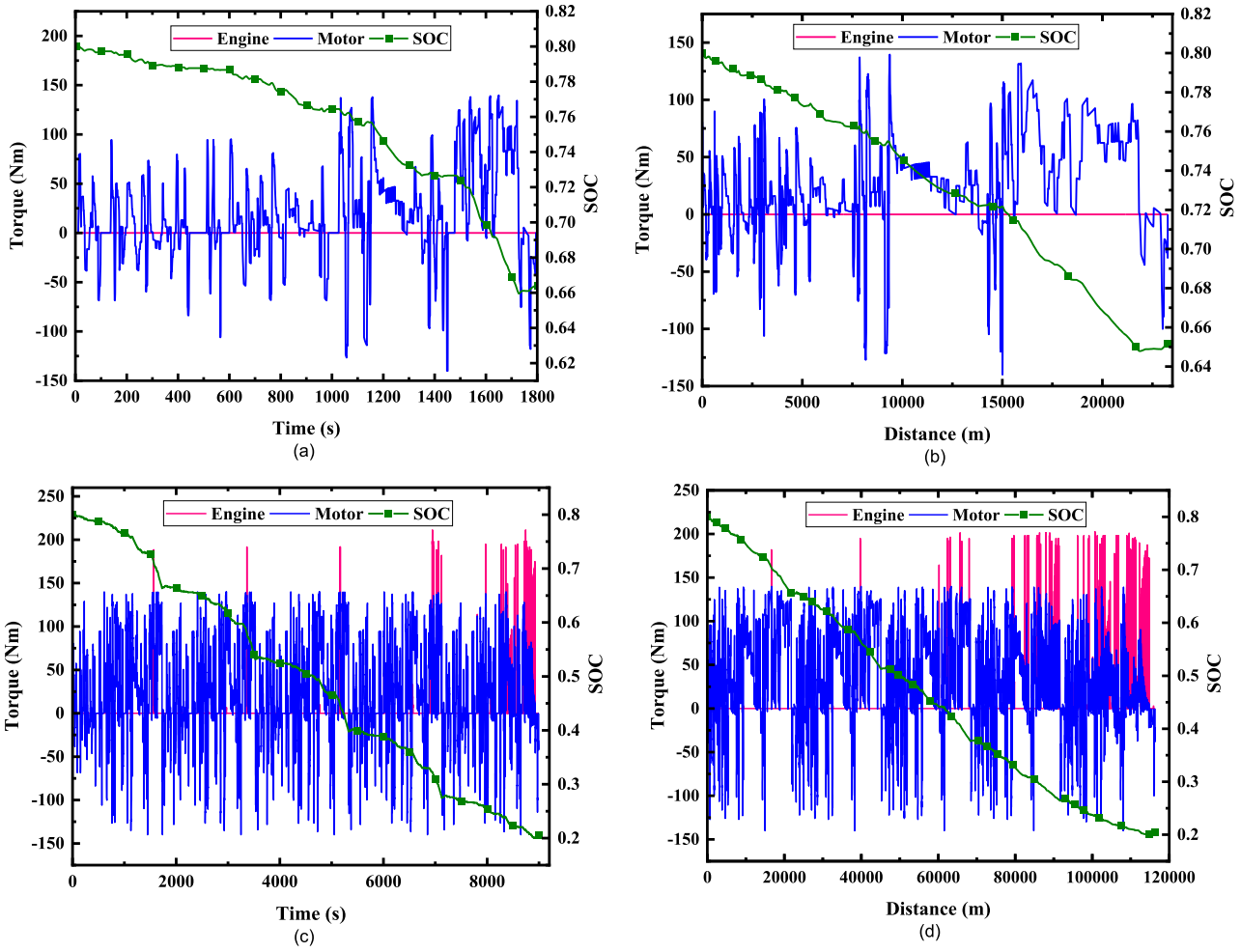

FIGURE 16. Engine, motor torque and SOC curves. (a) 1 WLTC in Time. (b) 1 WLTC in Space. (c) 5 WLTC in Time. (d) 5 WLTC in Space.

TABLE 6. Space domain planning and hierarchical optimization cost analysis.

Control strategy	Fuel consumption	Electricity consumption	Costs	Distance	Time
	CNY	CNY	CNY	km	s
Cooperation optimization	14.40	7.90	22.28	116.33	8885
Hierarchical optimization	16.30	8.20	24.50	116.33	9000

optimization, the time-domain solution resulted in an 11.0% increase in the cost. The fuel consumption cost is dropped by 15%, and the power consumption cost is reduced by 2.5%. The space-domain solution results in a 9.0% increase in fuel economy. The fuel consumption cost is decreased by 11.6%, and the power consumption cost is decreased by 3.6%. According to TABLE 7, the engine operating points are also mostly in the efficient region within this lower limit selection range. The comparison of the two control strategies shows that the economy of the collaborative optimization is better than that of the hierarchical strategy.

The comparison results for the two cases with a lower adjustment factor of 0.90 and 0.98 are chosen as the lower limit of the collaborative optimization, and the results show the former exhibits better economy in both the temporal and space domains. But the number of miles driven in the time domain decreases and the length of time in the space domain increases which is not in line with the true requirements. The simulation results above α_l takes the value of 0.98 to show the economic advantage. The mileage driven in the time domain is not much less than the original mileage, the time consumption in the space domain is lower than in the hierarchical optimization. Therefore, the constraint factor

TABLE 7. Fuel consumption distribution range of engine operating point.

Control strategy	Specific fuel consumption(g/kWh) (Proportion)						Total
Fuel consumption range	<300	300-350	350-400	400-450	450-500	>500	
Hierarchical optimization	445 (0.76)	44 (0.08)	27 (0.04)	11 (0.02)	27 (0.04)	37 (0.06)	591
Cooperation optimization space domain	256 (0.45)	79 (0.14)	33 (0.05)	68 (0.12)	95 (0.16)	49 (0.08)	580
Cooperation optimization time domain	241 (0.44)	63 (0.12)	30 (0.05)	93 (0.17)	96 (0.17)	29 (0.05)	552

is set as 0.98 to well meet the design intent of the proposed strategy.

V. CONCLUSION

In this paper, a collaborative optimal control strategy for vehicle speed planning and torque distribution is designed with energy economy as the research goal. First, the DP algorithm is leveraged to solve the optimal sequence of variables for the cooperative control model. Second, the torque and speed are coupled to achieve the synergistic effect during the solution process. Then, the feasible domain of conventional speed is determined to enable the autonomous vehicle to choose the velocity reasonably and accomplish the power allocation. Finally, by adding adjustable factors of constraint to limit the upper and lower limits of the speed domain, the vehicle can complete the mileage objectives in a specified time. To comprehensively confirm its effectiveness, simulations are performed in the time and space domains, respectively. The simulation results show that the collaborative optimization based on vehicle speed planning can increase fuel economy by 11% and 9% in the time and space domains respectively, compared to a hierarchical optimization strategy.

Further research can consider adding emission control criteria on the basis of energy economy to form a multi-objective optimal control strategy. Moreover, the exploration of the synergistic coupling between multiple environmental factors and speed, as well as power allocation, remains more challenging by incorporating more traffic environment factors into the cooperative optimization control strategy.

REFERENCES

[1] S. Verma, S. Mishra, A. Gaur, S. Chowdhury, S. Mohapatra, G. Dwivedi, and P. Verma, "A comprehensive review on energy storage in hybrid electric vehicle," *J. Traffic Transp. Eng. English Ed.*, vol. 8, no. 5, pp. 621–637, Jan. 2021.

[2] F. Zhang, X. Hu, R. Langari, and D. Cao, "Energy management strategies of connected HEVs and PHEVs: Recent progress and outlook," *Prog. Energy Combustion Sci.*, vol. 73, pp. 235–256, Jul. 2019.

[3] A. K. Tyagi and S. U. Aswathy, "Autonomous intelligent vehicles (AIV): Research statements, open issues, challenges and road for future," *Int. J. Intell. Netw.*, vol. 2, pp. 83–102, Jan. 2021.

[4] C. N. Gnanaprakasam, S. Meena, M. Nivethitha Devi, N. Shanmugasundaram, and S. Sridharan, "Robust energy management technique for plug-in hybrid electric vehicle with traffic condition identification," *Appl. Soft Comput.*, vol. 133, Jan. 2023, Art. no. 109937.

[5] S. Xie, X. Hu, T. Liu, S. Qi, K. Lang, and H. Li, "Predictive vehicle-following power management for plug-in hybrid electric vehicles," *Energy*, vol. 166, pp. 701–714, Jan. 2019.

[6] Y. Wang, X. Wang, Y. Sun, and S. You, "Model predictive control strategy for energy optimization of series-parallel hybrid electric vehicle," *J. Cleaner Prod.*, vol. 199, pp. 348–358, Oct. 2018.

[7] A. S. Mohammed, S. M. Atnaw, A. O. Salau, and J. N. Eneh, "Review of optimal sizing and power management strategies for fuel cell/battery/super capacitor hybrid electric vehicles," *Energy Rep.*, vol. 9, pp. 2213–2228, Dec. 2023.

[8] V. Larsson, R. Arvidsson, A. Westerlund, and N. Åkerblom, "Dynamometer test of a rule-based discharge strategy for plug-in hybrid electric vehicles," *IFAC-PapersOnLine*, vol. 49, no. 11, pp. 141–146, 2016.

[9] L. Yang, W. Wang, C. Yang, X. Du, and W. Zhang, "Online mixed-integer optimal energy management strategy for connected hybrid electric vehicles," *J. Cleaner Prod.*, vol. 374, Nov. 2022, Art. no. 133908.

[10] N. Xu, "Determination of vehicle working modes for global optimization energy management and evaluation of the economic performance for a certain control strategy," *Energy*, vol. 251, Jul. 2022, Art. no. 123825.

[11] N. Xu, Y. Kong, J. Yan, Y. Zhang, Y. Sui, H. Ju, H. Liu, and Z. Xu, "Global optimization energy management for multi-energy source vehicles based on 'Information layer–physical layer–energy layer–dynamic programming' (IPE-DP)," *Appl. Energy*, vol. 312, Apr. 2022, Art. no. 118668.

[12] J. Peng, H. He, and R. Xiong, "Rule based energy management strategy for a series–parallel plug-in hybrid electric bus optimized by dynamic programming," *Appl. Energy*, vol. 185, pp. 1633–1643, Jan. 2017.

[13] X. Lü, S. Li, X. He, C. Xie, S. He, Y. Xu, J. Fang, M. Zhang, and X. Yang, "Hybrid electric vehicles: A review of energy management strategies based on model predictive control," *J. Energy Storage*, vol. 56, Dec. 2022, Art. no. 106112.

[14] Z. Wei and Y. Zhang, "Intelligent ECMS for connected plug-in hybrid electric vehicles," *IFAC-PapersOnLine*, vol. 54, no. 10, pp. 278–283, Jan. 2021.

[15] Z. Chen, H. Gu, S. Shen, and J. Shen, "Energy management strategy for power-split plug-in hybrid electric vehicle based on MPC and double Q-learning," *Energy*, vol. 245, Apr. 2022, Art. no. 123182.

[16] Y. Liu, J. Zhao, S. Li, P. Dong, S. Wang, and X. Xu, "Adaptive energy management for plug-in hybrid electric vehicles considering real-time traffic information," *IFAC-PapersOnLine*, vol. 54, no. 10, pp. 138–143, 2021.

[17] Q. Guo, Z. Zhao, P. Shen, X. Zhan, and J. Li, "Adaptive optimal control based on driving style recognition for plug-in hybrid electric vehicle," *Energy*, vol. 186, Nov. 2019, Art. no. 115824.

[18] X. Lin, K. Li, and L. Wang, "A driving-style-oriented adaptive control strategy based PSO-fuzzy expert algorithm for a plug-in hybrid electric vehicle," *Exp. Syst. Appl.*, vol. 201, Sep. 2022, Art. no. 117236.

[19] Y. Zhang, X. Chen, J. Wang, Z. Zheng, and K. Wu, "A generative car-following model conditioned on driving styles," *Transp. Res. C, Emerg. Technol.*, vol. 145, Dec. 2022, Art. no. 103926.

[20] L. Lu, Y. Lin, Y. Wen, J. Zhu, and S. Xiong, "Federated clustering for recognizing driving styles from private trajectories," *Eng. Appl. Artif. Intell.*, vol. 118, Feb. 2023, Art. no. 105714.

[21] L. Hu, Q. Tian, C. Zou, J. Huang, Y. Ye, and X. Wu, "A study on energy distribution strategy of electric vehicle hybrid energy storage system considering driving style based on real urban driving data," *Renew. Sustain. Energy Rev.*, vol. 162, Jul. 2022, Art. no. 112416.

[22] P. Dong, J. Zhao, X. Liu, J. Wu, X. Xu, Y. Liu, S. Wang, and W. Guo, "Practical application of energy management strategy for hybrid electric vehicles based on intelligent and connected technologies: Development stages, challenges, and future trends," *Renew. Sustain. Energy Rev.*, vol. 170, Dec. 2022, Art. no. 112947.
[23] Y. Liu, Z. Huang, J. Li, M. Ye, Y. Zhang, and Z. Chen, "Cooperative optimization of velocity planning and energy management for connected plug-in hybrid electric vehicles," *Appl. Math. Model.*, vol. 95, pp. 715–733, Jul. 2021.
[24] Y. Liu, B. Huang, Y. Yang, Z. Lei, Y. Zhang, and Z. Chen, "Hierarchical speed planning and energy management for autonomous plug-in hybrid electric vehicle in vehicle-following environment," *Energy*, vol. 260, Dec. 2022, Art. no. 125212.
[25] L. Zhang, W. Liu, and B. Qi, "Energy optimization of multi-mode coupling drive plug-in hybrid electric vehicles based on speed prediction," *Energy*, vol. 206, Sep. 2020, Art. no. 118126.
[26] N. Guo, X. Zhang, Y. Zou, L. Guo, and G. Du, "Real-time predictive energy management of plug-in hybrid electric vehicles for coordination of fuel economy and battery degradation," *Energy*, vol. 214, Jan. 2021, Art. no. 119070.
[27] M. Zandie, H. K. Ng, S. Gan, M. F. Muhamad Said, and X. Cheng, "Multi-input multi-output machine learning predictive model for engine performance and stability, emissions, combustion and ignition characteristics of diesel–biodiesel-gasoline blends," *Energy*, vol. 262, Jan. 2023, Art. no. 125425.
[28] Z. Lei, D. Qin, L. Hou, J. Peng, Y. Liu, and Z. Chen, "An adaptive equivalent consumption minimization strategy for plug-in hybrid electric vehicles based on traffic information," *Energy*, vol. 190, Jan. 2020, Art. no. 116409.
[29] J. Koko, "Fast MATLAB assembly of FEM matrices in 2D and 3D using cell-array approach," *Int. J. Model., Simul., Sci. Comput.*, vol. 7, no. 2, Jun. 2016, Art. no. 1650010.

ZHENZHEN LEI (Member, IEEE) received the M.S. degree in automotive system engineering from the University of Michigan–Dearborn, Dearborn, MI, USA, in 2009, and the Ph.D. degree in mechanical engineering from Chongqing University, Chongqing, China, in 2019.

She is currently an Associate Professor of mechanical and power engineering with the Chongqing University of Science and Technology, Chongqing. She has conducted more than 15 projects and published more than 20 peer-reviewed journal articles and conference proceedings. Her research interests include energy management of plug-in hybrid electric vehicles and optimal control of intelligent electric vehicles.

YAFANG HUANG received the B.S. degree in automobile-service engineering from Nanyang Normal University, Nanyang, China, in 2020. She is currently pursuing the M.S. degree in resources and environment with the Chongqing University of Science and Technology, Chongqing, China.

Her research interest includes energy management strategies for clean energy vehicles.

SHUAI ZHANG received the B.S. degree in mechanical design manufacture and automation from the Qinggong College, North China University of Science and Technology, Tangshan, China, in 2017. He is currently pursuing the M.S. degree in resources and environment with the Chongqing University of Science and Technology, Chongqing, China.

His research interest includes energy management strategies for clean energy vehicles.

WENJUN WAN received the B.S. degree in communication engineering from the Nanchang Institute of Technology, Nanchang, China, in 2022. He is currently pursuing the M.S. degree in resources and environment with the Chongqing University of Science and Technology, Chongqing, China.

His research interest includes energy management strategies for clean energy vehicles.

YI SUI received the M.S. degree in chemical process equipment from the Lanzhou University of Technology, Lanzhou, China, in 2007.

He was a Technical Director of Chongqing Lifan Passenger Vehicle Company Ltd., from 2009 to 2015. Since 2016, he has been a Laboratory Assistant with the Automotive Service Engineering Experimental Teaching Center, Chongqing University of Science and Technology, Chongqing, China. He has conducted more than ten projects and has published more than ten journal articles. His research interests include control and application of battery energy management systems, motor drive control systems, and control and application of vehicle power transmission.

YONGGANG LIU (Senior Member, IEEE) received the B.S. and Ph.D. degrees in automotive engineering from Chongqing University, Chongqing, China, in 2004 and 2010, respectively.

He was a Joint Ph.D. Student and a Research Scholar with the University of Michigan–Dearborn, Dearborn, MI, USA, from 2007 to 2009. He is currently a Professor with the College of Mechanical and Vehicle Engineering, Chongqing University. He has leaded more than 30 research projects, such as the National Natural Science Foundation of China and the National Key Research and Development Program of China. He has published more than 90 research journal articles. His research interests include optimization and control of intelligent electric and hybrid vehicles and integrated control of vehicle automatic transmission systems. He is also a Senior Member of the China Society of Automotive Engineering.